MM Science Journal | www.mmscience.eu
ISSN 1803-1269 (Print) | ISSN 1805-0476 (On-line)
Special Issue | HSM 2025
18th International Conference on High Speed Machining
October 15-16, 2025, Prague, Czech Republic
DOI: 10.17973/MMSJ.2025_12_2025154

HSM2025-44823

ESTIMATION OF HARDNESS AND RESIDUAL STRESS OF MACHINED SURFACES USING IN-PROCESS DATA OBTAINED FROM TURNING OPERATIONS

Kazunori KOHARA[1], Yukio TAKAHASHI[1], Norikazu SUZUKI[2]*
[1]Chuo University, Department of Precision Mechanics, Tokyo, Japan
[2]Kobe University, Department of Mechanical Engineering, Hyogo, Japan
*Corresponding author; e-mail: nsuzuki@mech.kobe-u.ac.jp

Abstract
This study proposes a method to estimate the surface hardness and residual stress of carbon steel in turning by using analytical information of the cutting process. The machined surface properties depend on the strain, strain rate, stress and temperature fields generated during cutting. Therefore, these state conditions are estimated from the cutting force using a three-dimensional cutting model, and the hardness and residual stress are estimated using a linear regression model. The analytical results clarified that the hardness and residual stress could be estimated accurately.

Keywords:
Turning, force model, residual stress, surface hardness, tool wear, carbon steel

1 INTRODUCTION

The mechanical properties of the product, including fatigue strength, are determined by the hardness and residual stress of the material surface [Garwood 1951] [Sasahara 2005]. Consequently, strict control is imperative. In a previous study by Fujii et al., stress and temperature were estimated by applying an inverse analysis based on a cutting force model to cutting force and tool wear width measurements taken through end milling. [Fujii 2023]. The method is predicated on the assumption of a highly simplified linear regression model. In the case of turning, the three-dimensional nature of the process must be considered, as it differs from a process in which the finished surface coincides with the machined area where work is done by the main cutting edge, as in the case of end milling. In this study, shear strain, shear strain rate, stress field, and cutting temperature are estimated from the cutting process through verification experiments, and an attempt is made to estimate hardness and residual stress in turning using a linear regression model as in previous studies. Since cutting temperature and shear angle estimation based on shear angle theory are subject to inaccuracy, this study examined the effect of modelling errors in the turning process on the accuracy of hardness and residual stress estimation by comparing the results with actual measurements of cutting temperature and shear angle.

2 HARDNESS AND RESIDUAL STRESS ESTIMATION MODEL

2.1 Residual stress estimation model

Cutting operations generate extremely large strains and stresses in the shear region. In addition, the surface of the work piece is subjected to a thermal history specific to cutting. This changes the dislocation density and crystal structure of the workpiece surface, causing residual stresses [Henrisksen 1951][Brinksmeier 1982]. In this study, the stress and temperature in the work piece during machining are assumed to have a linear relationship with the residual stress on the finished surface, and the residual stress is estimated using the regression model shown in Equation (1). The coefficient vectors are identified from the experimental residual stresses using the least-squares method.

$$\begin{bmatrix} RS_1 \\ \vdots \\ RS_n \end{bmatrix} = \begin{bmatrix} \tau_{sr1} & \tau_{sf1} & \sigma_{sf1} & T_{psz1} & 1 \\ \vdots & \vdots & \vdots & \vdots & \vdots \\ \tau_{srn} & \tau_{sfn} & \sigma_{sfn} & T_{pszn} & 1 \end{bmatrix} \begin{bmatrix} a_0 \\ a_1 \\ a_2 \\ a_3 \\ RS_0 \end{bmatrix} \quad (1)$$

$\tau_{sr}, \tau_{sf}, \sigma_{sf}, T_{psz}$ are the shear stress on the shear face, shear stress on the flank, compressive stress on the flank, and temperature in the primary shear zone [Oxley 1989] [Ozel 2006], respectively. In this study, various state quantities are obtained by estimating shear angle and edge force based on shear angle theory and mechanistic model from the measured cutting force. Shear stress is determined by dividing the shear force by the shear area. Shear stress is shown in equation 2, where R is the

resultant cutting force, ϕ is the shear angle, b is the undeformed chip thickness, and d is the cutting width. The flank stress can be estimated from the measured flank wear width as the average stress occurring at the flank. The flank stress is obtained by dividing the edge force by the contact area between the workpiece and the tool flank. Equation 3 shows the stress on flank with edge force coefficient in cutting direction K_{ep}, edge force coefficient perpendicular to flank K_{ef} and width of flank wear l_{VB}. The primary shear zone temperature is obtained as the sum of the temperature rise due to shear force F_s work multiplied by the workpiece inflow rate λ and the room temperature T_0. The primary shear zone temperature is shown in equation 4 with the density of the workpiece as ρ and specific heat of workpiece as S. Density and specific heat are assumed to be constant, although they vary with temperature. In this study, the estimation accuracy using estimated cutting temperature is compared to the estimation accuracy using measured cutting temperature for model validation. In this study, the estimation accuracy using estimated shear angle obtained from shear angle theory is compared to the estimation accuracy using estimated shear angle obtained from chip thickness measurements.

$$\tau_{sr} = \frac{R\cos(\phi + \beta - \alpha)}{bd/\sin(\phi)} \tag{2}$$

$$\tau_{sf} = \frac{K_{ep}}{l_{VB}}, \sigma_{sf} = \frac{K_{ef}}{l_{VB}} \tag{3}$$

$$T_{psz} = \frac{(1-\lambda)F_s\cos(\alpha)}{\rho S b d \cos(\phi - \alpha)} + T_0 \tag{4}$$

2.2 Hardness estimation model

It is known that there is a linear relationship between the hardness and yield stress of metals [Tabor 1948]. In this study, we assumed that the yield stress of polycrystalline materials σ_y can be estimated based on the Hall-Petch equation (5). In the Hall-Petch equation, k_y is the strengthening coefficient, σ_0 is the starting stress for dislocation movement. It has been documented that σ_0 exhibits a strain rate dependence[Miura 1998]. In this study, it is assumed that there is a quadratic relationship between σ_0 and the shear strain rate $\dot{\gamma}$, as shown in equation (6). A method of grain size d refinement by large strain processing is known. It has been reported that this effect is temperature dependent [Maki 2014]. In this study, $d^{-1\backslash 2}$ is assumed to be related to the primary shear zone temperature T_{psz} and shear strain γ as shown in equation (7). It has been reported that there is a linear relationship between shear strength and Vickers hardness [Zhang 2011] and between residual stress and Vickers hardness [Kagawa 1990]. The yield stress σ_y expressed as the sum of equations (6) and (7), shear stress τ_{sr} and residual stress RS were assumed to have a linear relationship with hardness HV. The linear regression model shown in equation (8) was used to estimate hardness. Residual stress RS was the average of the axial and circumferential residual stress of workpieces estimated in Section 2.1. Shear strain and shear strain rate can be determined from work material properties and machining conditions [Oxley 1989] [Ozel 2006]. The strain γ and strain rate $\dot{\gamma}$ are shown in equation (9) and (10) with shear rate V_s, shear length l and strain rate constant C_0.

$$\sigma_y = \sigma_0 + k_y d^{-\frac{1}{2}} \tag{5}$$

$$\sigma_0 = A_1\dot{\gamma}^2 + A_2\dot{\gamma} + A_3 \tag{6}$$

$$\frac{1}{\sqrt{d}} = B_1\gamma + B_2\sqrt{T_{psz}} + B_3 \tag{7}$$

$$\begin{bmatrix} HV_1 \\ \vdots \\ HV_n \end{bmatrix} = \begin{bmatrix} \sigma_{y1} & \tau_{sr1} & RS_1 & 1 \\ \vdots & \vdots & \vdots & \vdots \\ \sigma_{yn} & \tau_{srn} & RS_n & 1 \end{bmatrix} \begin{bmatrix} b_0 \\ b_1 \\ b_2 \\ HV_0 \end{bmatrix}$$

$$= \begin{bmatrix} \dot{\gamma}_1{}^2 & \dot{\gamma}_1 & \sqrt{\gamma_1} & \sqrt{T_{psz1}} & \tau_{sr1} & RS_1 & 1 \\ \vdots & \vdots & \vdots & \vdots & \vdots & \vdots & \vdots \\ \dot{\gamma}_n{}^2 & \dot{\gamma}_n & \sqrt{\gamma_n} & \sqrt{T_{pszn}} & \tau_{srn} & RS_n & 1 \end{bmatrix} \begin{bmatrix} c_0 \\ c_1 \\ c_2 \\ c_3 \\ c_4 \\ c_5 \\ HV_0 \end{bmatrix} \tag{8}$$

$$\gamma = \frac{\cos(\alpha)}{2\sin(\phi)\cos(\phi - \alpha)} \tag{9}$$

$$\dot{\gamma} = C_0\frac{V_s}{l} \tag{10}$$

3 EXPERIMENTAL METHOD

Turning experiments were conducted on a carbon steel (S45C) round bar using a turning center (Okuma, MULTUS B200). Fig. 1 shows the appearance of the experimental setup and Tab. 1 shows the conditions of the cutting experiment. The rake angle is 0° and the depth of cut is 1 mm for all conditions. Cutting force during machining was measured with a dynamometer (Kistler, 9129A), and cutting temperature was measured with a tool workpiece thermocouple method. Fig. 2 shows the calibration curve for the thermocouple. The hardness and residual stress corresponding to each feed condition were measured. The hardness of the surface was determined as the average value of five points measured using a micro-Vickers hardness tester (Shimadzu, HMVG-31). Tool marks were polished using sandpaper by approximately 10 μm, and hardness was measured at five points to reduce the influence of measurement errors. Surface residual stress was measured in the axial and circumferential directions of the workpiece using an X-ray residual stress analyzer (PULSTEC, μ-360X). In order to minimize the effect of measurement errors, residual stress was measured at four equally spaced points along the same circumference. Residual stress was measured avoiding the polished areas. Fig. 3 shows the measurement points for hardness and residual stress.

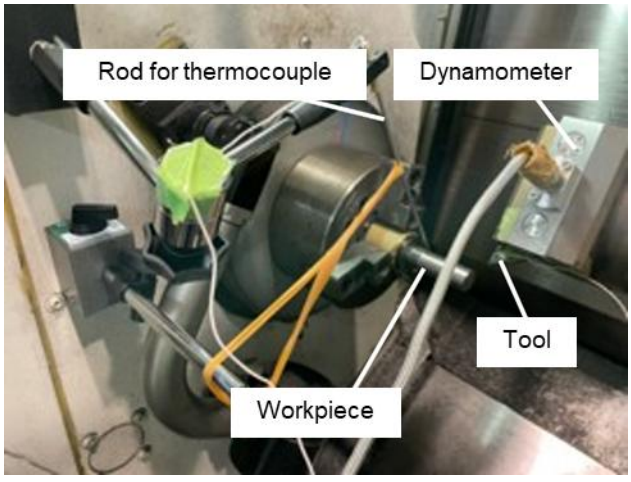

Fig. 1: Experimental setup

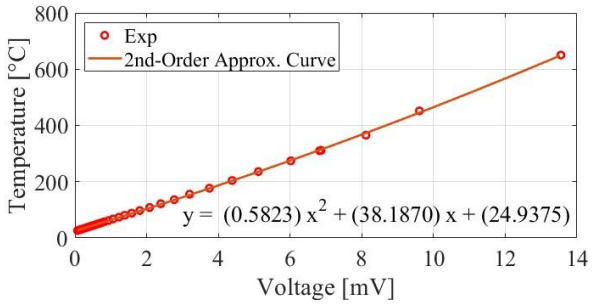

Fig. 2: Thermocouple calibration curve

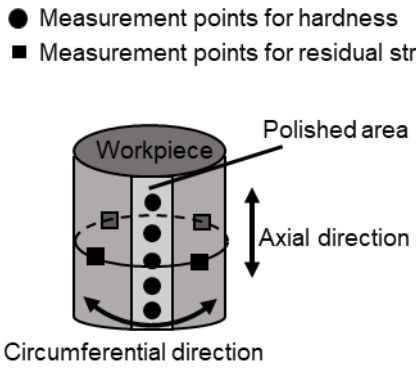

Fig. 3: Measurement points for hardness and residual stress

Tab. 1: Cutting condition

	#1	#2	#3	#4
Machine tool	MULTUS B200			
Cutting tool	Cemented Carbide Non-coated DCGW11T302R			
Workpiece	S45C			
Atmosphere	DRY			
Feed rate [mm/rev]	0.1 0.125 0.15 0.175 0.2			
Depth of cut [mm]	1			
Nose radius [mm]	0.2	0.2	0.2	**0.4**
Cutting speed [m/min]	120	120	**180**	120
Cutting distance [m]	113	**281**	119	123

4 EXPERIMENTAL RESULTS AND CONSIDERATIONS

To investigate the effect of modeling error on the shear angle, Fig. 4 shows the relationship between the measured shear angle determined from the chip thickness and the shear angle estimated from the maximum shear stress theory. Fig. 5 shows the relationship between the primary plasticity zone temperature determined from the measured shear angle and the primary shear zone temperature determined from the estimated shear angle. In Fig. 4, the horizontal axis is the shear angle determined from the chip thickness (hereinafter, this is called 'measured shear angle' or 'measured ϕ') and the vertical axis is the shear angle determined from the maximum shear stress theory (hereinafter, this is called 'estimated shear angle' or 'estimated ϕ'). In Fig. 5, the horizontal axis is the primary shear zone temperature determined from the measured shear angle and the vertical axis is the primary shear zone temperature determined from the estimated shear angle.The results are plotted when the feed rate is 0.15 [mm/rev], respectively.

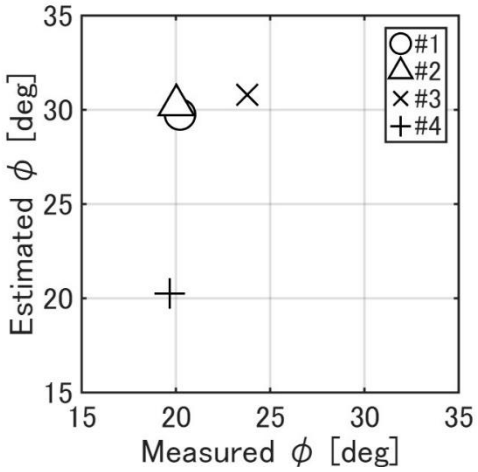

Fig. 4: Result of shear angle at a feed rate of 0.15

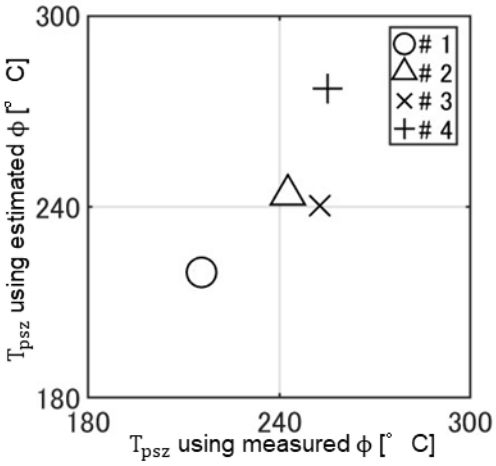

Fig. 5: Result of primary shear zone temperature at a feed rate of 0.15

Fig. 4 and Fig. 5 show that there is a large difference between the measured and estimated values of the shear angle, and that the error in the primary shear zone temperature is large accordingly. On the other hand, the trend of the variation of the measured and estimated shear angles with respect to the experimental conditions is generally consistent, and the same trend can be confirmed for the primary shear zone temperature.It was confirmed that the trends were generally the same except for the feed rate of 0.15 [mm/rev]. Fig. 6 shows hardness result and Fig. 7 shows residual stress result. Fig. 6 and Fig. 7 shows that the hardness and residual stress varies depending on the feed rate and experimental conditions.

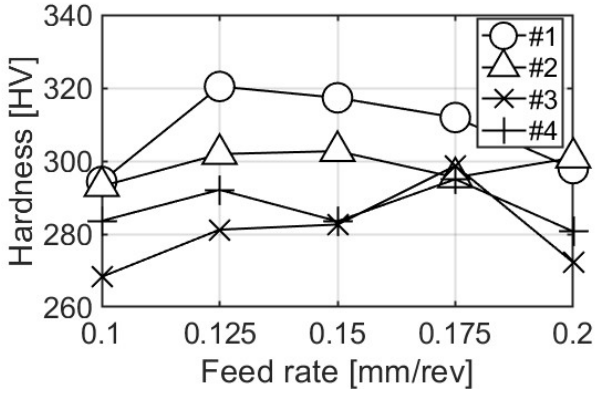

Fig. 6: Hardness results

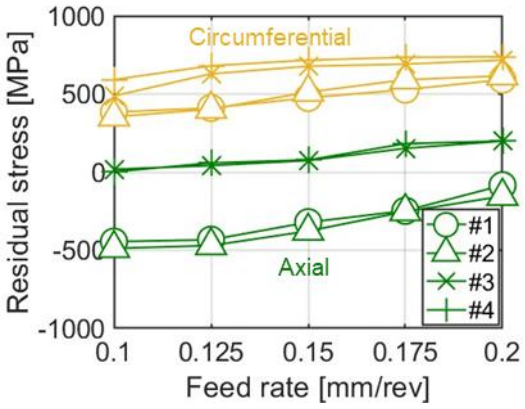

Fig. 7: Residual stress results

Fig. 8 shows hardness estimation result and Fig. 9 shows residual stress estimation result. Both were estimated using estimated shear angle and primary shear zone temperature determined from estimated shear angle. The horizontal axis is the measured value and the vertical axis is the estimated value. In Fig. 9, yellow plots show the axial residual stresses and the green plots show the circumferential residual stresses in the workpiece.The coefficient of determination R^2 for evaluating the accuracy of the model estimation is shown in each figure. In Fig. 8 and Fig. 9, the coefficients of determination for hardness and residual stress are greater than 0.7 and 0.9, respectively, indicating that the estimation accuracy is high.

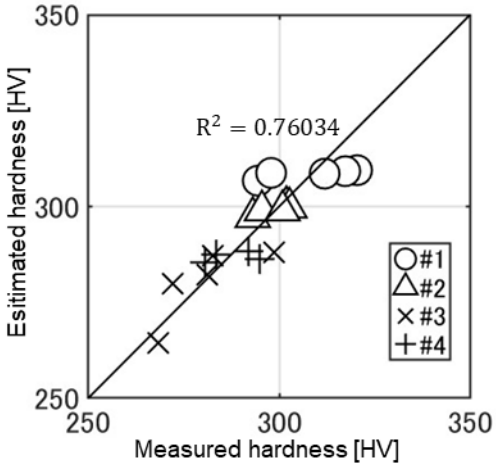

Fig. 8: Hardness estimation result

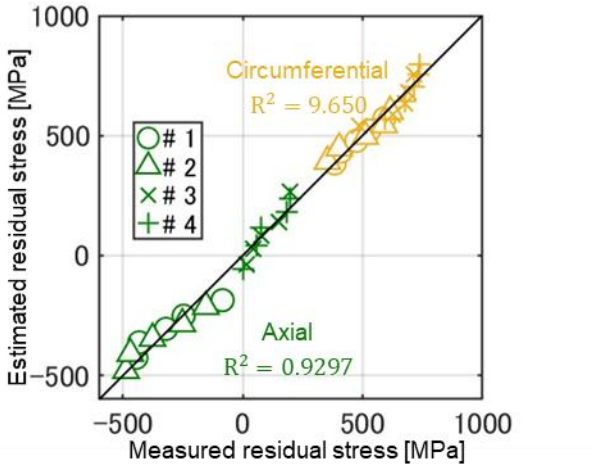

Fig. 9: Residual stress estimation result

Fig. 10 shows a comparison of the coefficients of determination for hardness and residual stress estimation when using measured versus estimated values. The vertical axis is the coefficient of determination, the horizontal axis is the hardness HV, the axial residual stress RSa of the workpiece, and the circumferential residual stress RSc of the workpiece. The blue bars show the results using cutting temperature measured by tool workpiece thermocouple method (hereinafter, this is called 'measured cutting temperature', or 'measured T') and measured shear angle. The orange bars show the results using primary shear zone temperature (hereinafter, this is called 'estimated cutting temperature' or 'estimated T') and measured shear angle. The yellow bars show the results using measured cutting temperature and measured shear angle. The purple bars show the results using estimated cutting temperature and shear angle. In Fig. 10, estimation accuracy using estimated cutting temperature is higher than using measured cutting temperature. Although there is an effect of modeling error in the shear angle, the coefficients of determination do not differ significantly. As shown in Fig. 4 and Fig. 5, the modeling error of the shear angle affects each explanatory variable, but this is thought to be because the trends of each explanatory variable are consistent between the measured and estimated values.

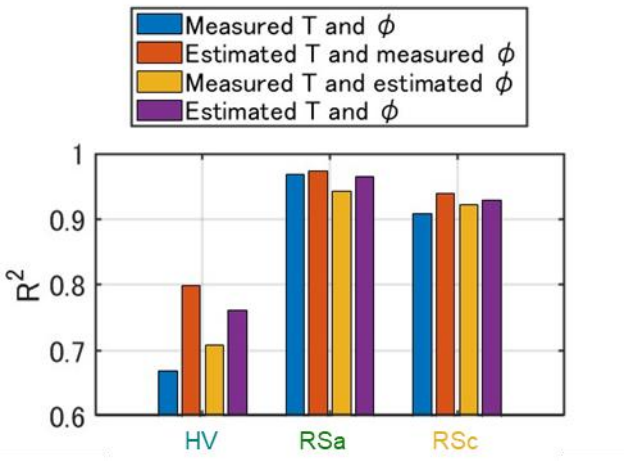

Fig.10: Comparison of coefficients of determination

5 CONCLUSION

In this study, a method for estimating hardness and residual stress using cutting force analysis was proposed and

verified the accuracy and validity of the model by turning experiments. The effect of process modeling error on estimation accuracy was also analyzed by comparing the estimation results using measured shear angle and measured cutting temperature with those using estimated values. Validation experiments confirmed that hardness and residual stress can be accurately estimated by the proposed model. The accuracy of estimation using estimated cutting temperature is higher than using measured cutting temperature, and modeling errors in shear angle estimation had little effect on the accuracy of hardness and residual stress estimation.

6 REFERENCES

Paper in a journal:

[Brinksmeier 1982] E. Brinksmeier et al., Residual stresses—measurement and causes in machining process, Ann. CIRP, 1982, Vol.31, pp.491-509.

[Fujii 2023] T. Fujii et al., Estimation of Hardness and Residual Stress on End-Milled Surfaces Using Linear Regression Model, International Journal of Automation Technology, 2023, Vol.17, No.6, pp. 564-574.

[Henriksen 1951] E.K. Henriksen, Residual stress in machined surface, Transaction ASME, 1951, Vol.73, No.1, pp.69-76.

[Kagawa 1990] K. Kagawa et al., A Method for the Residual Stress from Hardness Variations -Correlation of Elastic Stress and Vickers Microhardness, JSPE, 1990, 1698, pp.128-134.

[Miura 1998] K. Miura et al., Influence of Strain Rate on Grain Size Dependence of Strength of Sheet Steel, Journal of the Society of Materials Science Japan, 1998, Volume 47, No.10., pp.1053-1058.

[Ozel 2006] T. Özel, E. Zeren, A Methodology to Determine Work Material Flow Stress and Tool-Chip Interfacial Friction Properties by Using Analysis of Machining, Journal of Manufacturing Science and Engineering, Transactions of ASME, 2006, Vol.128, pp.119-129

[Sasahara 2005] H. Sasahara, The effect on fatigue life of residual stress and surface hardness resulting from different cutting conditions of 0.45%C steel, International Journal of Machine Tools & Manufacture, 2005, Vol.45, pp.131-136.

[Zhang 2011] P. Zhang et al., General relationship between strength and hardness, Materials Science and Engineering A, 2011, A529, pp.62-73.

Technical reports or thesis:

[Tabor 1948] D. Tabor, A simple theory of static and dynamic hardness, Proceedings of the Royal Society of London. Series A, Mathematical and Physical Sciences, 1948, Volume 192, Issue 1029, pp.247-274.

[Garwood 1951] M.F. Garwood, et al., Correlation of Laboratory tests and service performance. Interpretation of tests and correlation with service, American Society for Metals,1951, pp.1-77.

[Oxley 1989] Oxley, P.L.B., Mechanics of machining, an Analytical Approach to Assessing Machinability, Ellis Horwood Limited, 1989.

[Maki 2014] T. Maki et al., Thermomechanical Processing of Steel –Past, Present and Future–, Tetsu-to-Hagané, 2014, Vol. 100, No. 9., pp.14-27.